International Research Journal of Engineering and Technology (IRJET) e-ISSN: 2395-0056
Volume: 07 Issue: 04 | Apr 2020 www.irjet.net p-ISSN: 2395-0072

Comparative Analysis of Three Port DC-DC Converters for Stand-Alone Photovoltaic Systems for EV Charging

Sinha raviranjankumar[1], Nishit Joshi[2], Swapnil Patil[3], Shanu Shrivastav[4], Prof. Rahul Jadav[5]

[1-5]UG student, Assistant Professor, Electrical Engineering Department, Laxmi Institute of Technology, Sarigam

---

***Abstract*-** System efficiency and cost effectiveness are more important issues with photovoltaic systems. As the stand-alone systems are independent of grid, the front end converter which employed for power transfer should posses features like, high Step-Up ratio, Optimized Maximum Power point tracking and multiple operational modes. This paper addresses the two issues with stand-alone systems while making a comparative analysis of various topologies of three port DC-DC converters which are employed for different applications. For the performance verification of the converter a MATLAB model of photovoltaic module of 60W is simulated in MATLAB/SIMULINK environment for the converter integrity

***Index Terms*-**DC-DC power converter, stand alone systems

1. Introduction

As the manufacturing cost of photovoltaic panels is getting reduced continuously due to constant research on semiconductor devices and hence the utilization of solar power is gaining more popularity. Solar/ PV based power generation can be employed as Grid connected or Off Grid (Stand-Alone) systems [1].

Stand-alone systems are independent of utility grids and commonly employed in space application, unmanned aerial vehicles, remote communication systems, traffic signals and domestic application where grid integrity is difficult to achieve. For such systems it is necessary to provide a storage element like battery bank which can accommodate the intermittent power generation from PV modules [2].

Traditionally, The DC-DC converters are modeled as two port network topology and they can be half bridge or full bridges can support the multiport structure up to some extent [3]. A modified half bridge converter is discussed in [4]. Which comprises of one PV input port, one isolated output port and one intermediate bidirectional battery port to accommodate the intermittent power generation from photovoltaic systems.

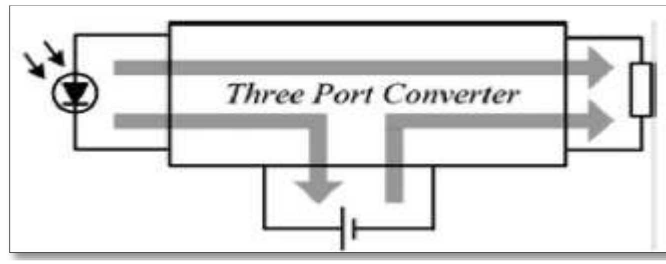

Figure 1- Stand-Alone system with Three port Converter

Fig.1 shows how energy of the stand-alone system is directed towards load and to the energy storage elements either it may be a battery of a super capacitor. Hence Three Port Converter found to be a best candidate that can provide better interface with source, the storage element and the load with the stand-alone system. A detailed analysis and comparison has been given in [6], which indicates that employing TPC with stand-alone systems has advantages such as high system efficiency, compact single unit solution, lower cost, faster response and centralized control scheme. Due to these noticeable merits, these converters have become very popular for various applications Based on the detailed analysis and study of different topologies, a comparative analysis of most commonly utilized three port DC-DC converters is carried out in this paper. In section II, The basic description of converter topology, its operational modes and control scheme is discussed. In section III, Simulation results of all the topologies with PV module of 60 W rating which are simulated in MATLAB environments shown. In section IV, depending on the theoretical analysis and the simulation results a comparative statements in tabular format is described and finally, conclusion is given in section V.

2. Topologies and their operation

I. THREE PORT FULL BRIDGE CONVERTER

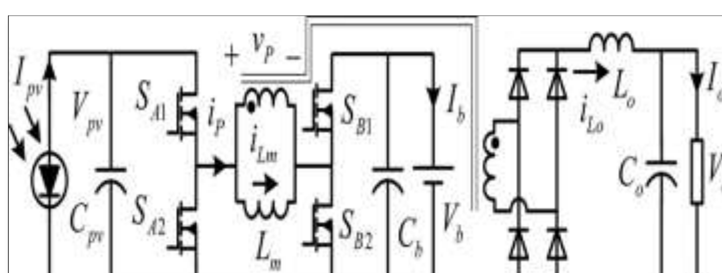

Figure 2 Full-Bridge Three Port DC-DC Converter

Fig.2 shows a FB-TPC which can be applied to Stand-alone photovoltaic systems which comprises of three ports which are PV module, a battery and an output port [7].

Energy can be diverted into three paths which are as follows: 1). From PV to load, 2). From PV to Battery and 3). From Battery to load

In Fig.2 (SA1, SA2) and (SB1, SB2) forms a bridge circuit of the converter which is connected in parallel with primary winding of the transformer and the magnetizing inductance of the transformer is lumped on the primary side. Now the voltage of the two sources will be Vsa and Vsb will be equal then they are connected in parallel which in turn forms the full bridge circuit.

As the output voltage at the load port is required to be tightly regulated to meet the load requirements and similarly at the input port the PV voltage required to have Maximum power tracking so that the maximum energy from the PV can be received form PV. Therefore, any mismatch occurs during the operation of the converter in either port, the load requirements should be fulfilled by the intermediate battery port.

This leads to the conclusion that any of the two ports of the FB-TPC should be controlled independently and hence required two independent measuring variables.

a) ANALYSIS OF THE FB-TPC

The analysis of the FB-TPC can be carried out depending on the operational modes of the converter illustrated in Table.1

Table 1- Operational modes and power flow of FB-TPC

Operational Modes	**Power of PV**	**Power of battery**
Dual- output mode	$P_{pv} \geq P_o$	Battery charging $P_b \geq 0$
Dual- input mode	$P_{pv} \leq P_o$, $P_{pv} > 0$	Battery discharging $P_b < 0$
Single input single output mode	$P_{pv} = 0$	Battery discharging $P_b = -P_o$

If the power loss in the converter is ignored then,

$$P_{pv} = P_o + P_b \quad (1)$$

Where P_{pv}, P_o and P_b are the powers flows form PV module, the output port and the battery respectively. There are three operational modes of FB-TPC are mentioned in Table1: 1) Dual-output (DO) mode, in which the P_{pv} is more than the P_o, hence the additional power is utilized to charge the battery. 2) Dual-input (DI) mode, in which the load power requirement is more than the generation by PV, at that time the battery supplies the load along with the PV. 3) Single Input Single Output (SISO) mode which reflects the night time operation of the converter (P_{pv}= 0) hence in this mode the battery caters the load. According to the modes of operation the Fig-3 reflects the power flow through the converter.

The switching signals to the switches are remains the same for all the operational modes of the converter as shown in Fig.5 but the only difference is the magnitude and the direction of i_{Lm} , which depends on the power P_{pv} and P_o as shown in Fig.3.

In DO mode the i_{Lm} is positive, In SISO mode the i_{Lm} is negative and in DI mode the i_{Lm} can be either positive or negative.

To analyze the converter performance we will discuss the DO mode. Before analyzing the operation of the converter following assumptions are taken into account:

- The capacitors C_{pv}, C_o and C_b are large enough so that V_{pv}, V_o and V_b can be considered constant during steady state.
- $V_{pv} \geq V_b$ case is analyzed for the switching signals

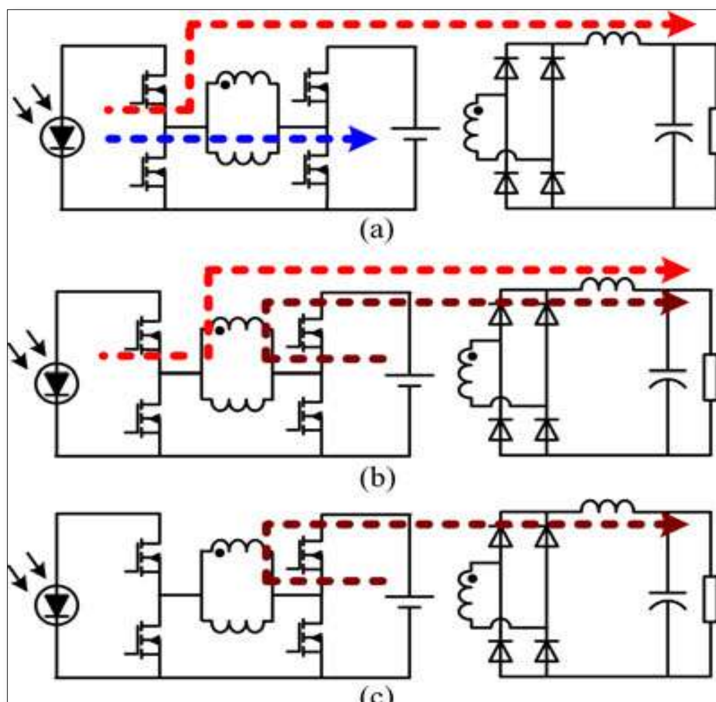

Figure 3- Power flow paths of each mode (a) DO mode (b) DI mode (c) SISO mode

There are four switching states are present in one cycle. The key waveform and equivalent circuit is shown in Fig.5 and Fig.6.

International Research Journal of Engineering and Technology (IRJET) e-ISSN: 2395-0056
Volume: 07 Issue: 04 | Apr 2020 www.irjet.net p-ISSN: 2395-0072

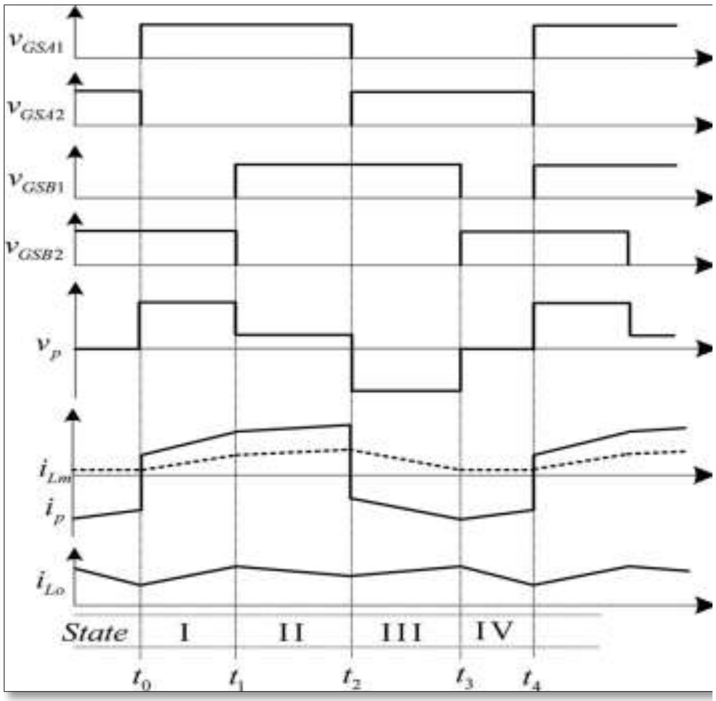

Figure 4- Key Waveforms of FB-TPC

State I: initially consider switches SA2 & SB2 are ON and SA1 & SB1 are OFF. At t0, SA1 turns ON & SA2 OFF. Then the voltage across the primary winding of transformer is positive.

$$\begin{cases} \frac{diLm}{dt} = \frac{Vpv}{Lm} \\ \frac{diLo}{dt} = \frac{nVpv - Vo}{Lo} \\ iP = iLm + niLo \end{cases} \quad (2)$$

State II: At t_1, S_{B2} turns OFF and S_{B1} turns ON. A positive voltage is applied on the primary winding of the transformer

$$\begin{cases} \frac{diLm}{dt} = \frac{(Vpv-Vb)}{Lm} \\ \frac{diLo}{dt} = \frac{n(Vpv - Vb) - Vo}{Lo} \\ iP = iLm + niLo \end{cases} \quad (3)$$

State III- [t_2-t_3]: At t_2, S_{A1} turns OFF and S_{A2} turns ON. A negative voltage is applied on the primary winding of the transformer

$$\begin{cases} \frac{diLm}{dt} = \frac{-Vb}{Lm} \\ \frac{diLo}{dt} = \frac{nVb - Vo}{Lo} \\ iP = iLm - niLo \end{cases} \quad (4)$$

State IV-[t3-t4]: At t3, SB 1 turns OFF and SB 2 turns ON. The voltage across the primary winding is clamped at zero, and iLm freewheels through SA2 and SB2.

$$\begin{cases} \frac{diLm}{dt} = 0 \\ \frac{diLo}{dt} = \frac{-Vo}{Lo} \end{cases} \quad (5)$$

Fig.5 depicts the equivalent circuit of the converter reflecting each switching state

Fig.6 illustrates the overall control scheme for the FB-TPC. Which containing four measuring variable and for that four regulators are employed. IVR for PV voltage regulation, BVR for battery voltage regulation, BCR for battery current regulation, OVR for output voltage regulation, the output of the regulators are applied to competitive mode selection block which produces the modulating waveform for the PWM modulators and the output of the PWM modulators are the gate signals for the switches.

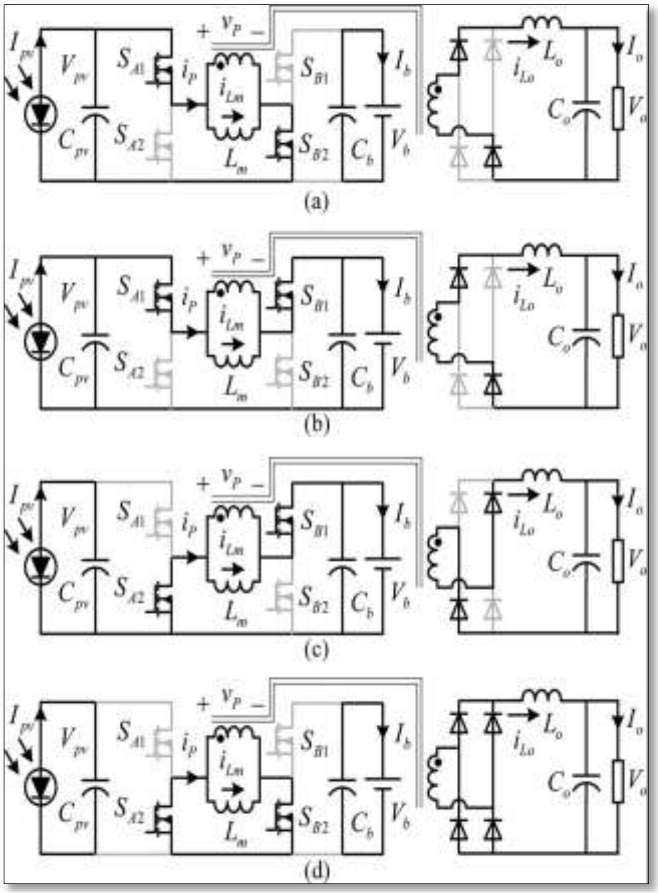

Figure 5- Equivalent circuit according to switching states (a) [t0-t1] (b) [t1-t2] (c) [t2-t3] (d) [t3-t4]

b) CONTROL SCHEME

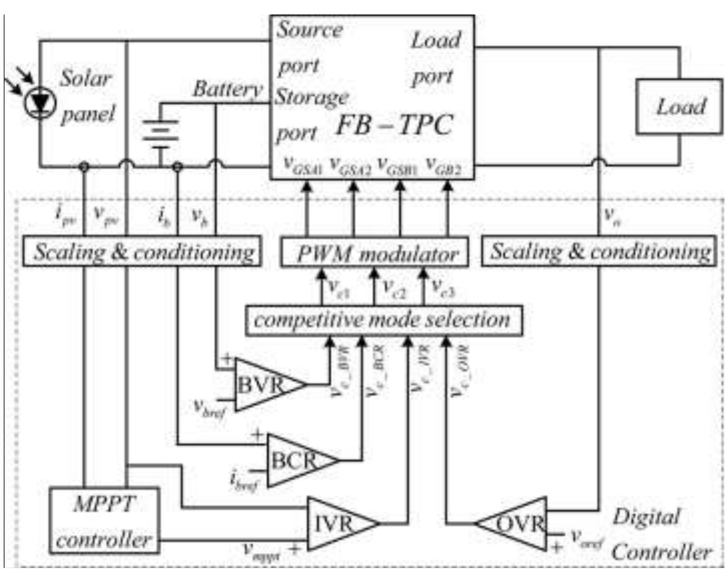

Figure 6- Control scheme of FB-TPC

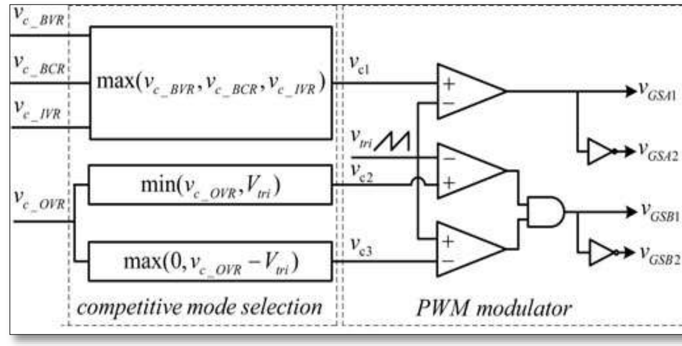

Figure 7- Mode selection block

Fig.8 shows the mode selection block in which the output signals of the regulator are employed and the output signal generated by following these set of equations:

$$\begin{cases} \text{Vc1: max (Vc\_BVR, Vc\_BCR, Vc\_IVR)} \\ \text{Vc2: min (Vc\_OVR, Vtri)} \\ \text{VC3: max (0, Vc\_OVR, -Vtri)} \end{cases} \quad (6)$$

3. THREE PORT MODIFIED HALF BRIDGE CONVERTER

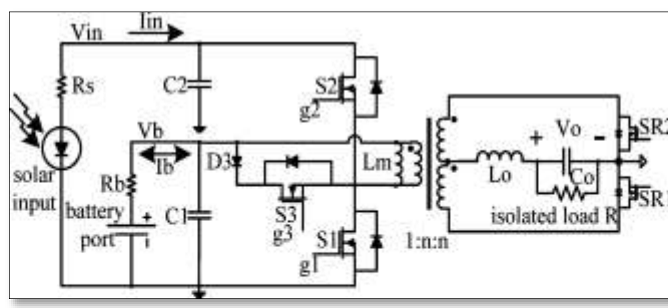

Figure 2- Three Port Modified Half Bridge Topology

Fig. 9 shows the modified Half Bridge three port converter which consists of three main switches S1, S2 and S3 working in the synchronous rectification mode to achieve ZVS operation [8]. There are only to control variables d1 and d2 for switches S1& S2 respectively and the third port is employed to have power balance. In this converter the C1 and C2 provided for the Battery and PV module are sufficiently large enough to ensure that at steady state the voltage of battery should be constant. A three winding high frequency transformer is employed to connect the source and the load. The magnetizing inductance of the transformer is lumped at the primary side of the converter.

a. ANALYSIS OF THE CONVERTER OPERATION

As the HB-TPC is employed for the satellite operation the converter for one orbit cycle is illustrated in Fig.10. For simplification of the analysis two assumptions are made: 1) Load power is to be constant. 2) Battery over-discharging is ignored as the PV modules and battery are oversized for safety margin

In stage I there is no insolation received hence the battery behaves as the primary source and during this period the battery state of charge is reduced.

In stage II which shows the initial insolation period, the power generation by PV module is not sufficient to supply the load, hence during this period the PV and Battery fulfill the load requirement. During this period the battery state of charge also gets reduced.

In stage III the full insolation received by the PV module. Power generation by the PV module is sufficient to supply the load and charge the battery. During this period the battery state of charge is increased.

In stage IV which is equivalent to stage II in which the battery and PV module cater the load. In this mode of operation battery charge control is provided to prevent the overcharging the battery which in turn increases the battery life.

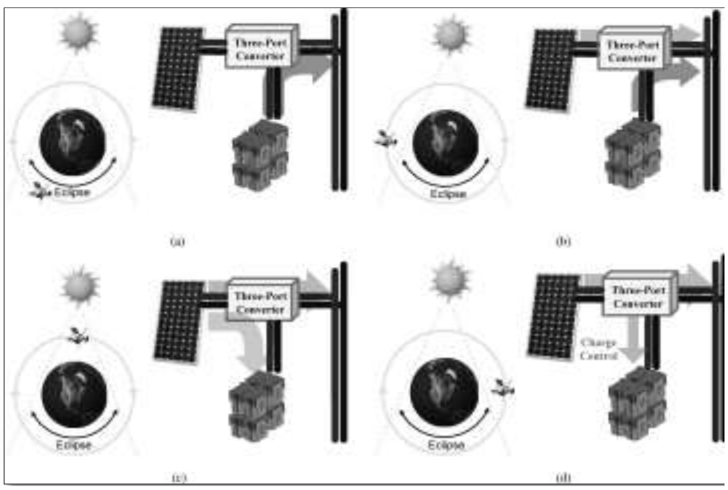

Figure 3- Different operational modes in one orbit cycle

a) CONTROL STRUCTURE

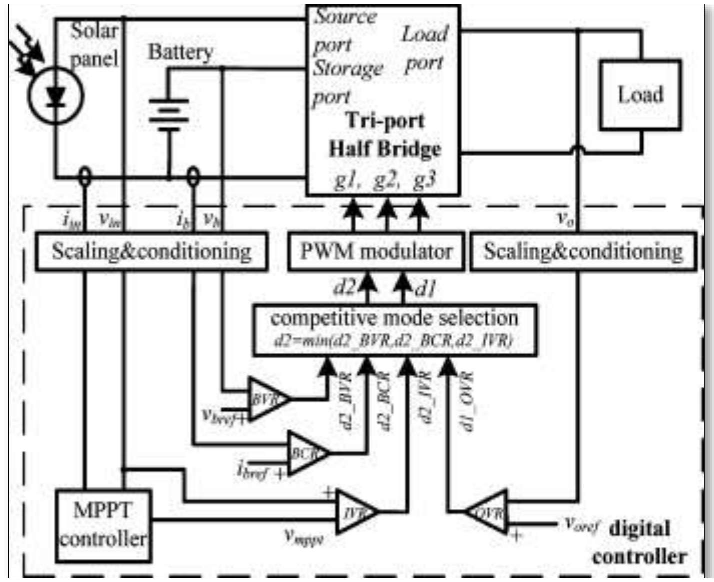

Figure 4- Control scheme for HB-TPC

Fig.11 shows the control structure for the HB-TPC, there are for regulators are used to control the converter operation as well as to achieve the seamless transition from one mode to another mode of the converter. From the output of the mode selection there are two controlling signals which make the control scheme complex, as overlapping comes into picture.

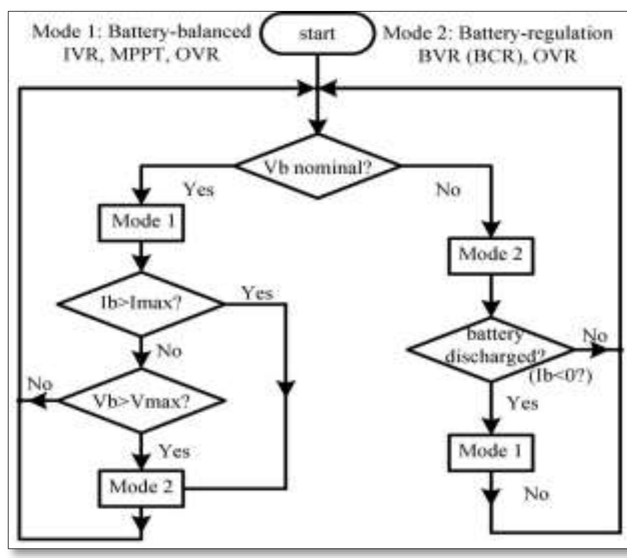

Figure 5- Mode selection algorithm

Fig.12 shows a flowchart to have transition between different modes of operation of the converter.

International Research Journal of Engineering and Technology (IRJET) e-ISSN: 2395-0056
Volume: 07 Issue: 04 | Apr 2020 www.irjet.net p-ISSN: 2395-0072

4. THREE PORT DC-DC CONVERTER DERIVED FROM FLYBACK AND FORWARD TOPOLOGY

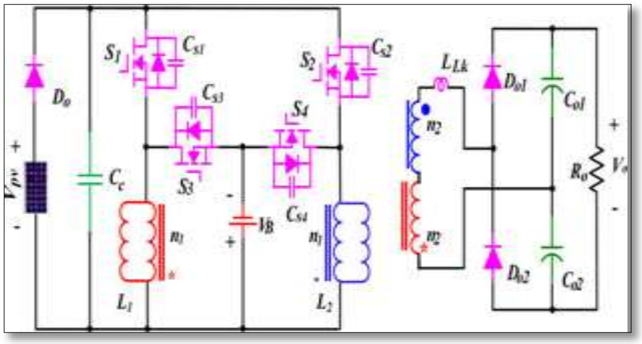

Figure 6-Three port DC-DC converter derived from Fly-Back and Forward topology

Fig. 13 shows a TPC derived from Fly-Back and Forward topology [8]. The switches S1 and S2 are the main switches that transfer energy from PV to battery of to load. Switch S3 and S4 are the auxiliary switches that transfer energy form source to load. L1 & L2 are the coupled inductors whose primary windings having n1 turns and secondary windings having n2 turn. The turns ratio N= (n2/n1) = 2.

Fig.13 describes the various modes of operations of the converter. In mode 1 which reflects the daytime operation the PV supplies the load or may be the battery depending up on the loading condition. In mode 2 which reflects the night time operation the battery supplies the load. In mode3 the load is disconnected and the energy generated by the PV is directed towards the battery to increase the state of charge of battery

For the analysis of the converter we will discuss the operational mode 1.

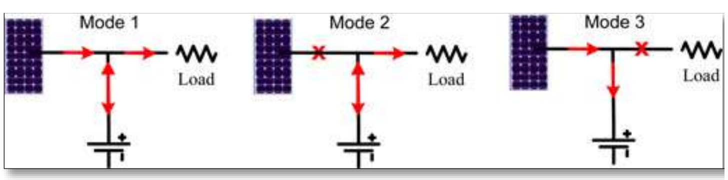

Figure 7- Operational modes of the converter

Fig.14 describes the key waveforms of the converter in Mode1. Where Vgs1, Vgs2, Vgs3 and Vgs4 are the gate signals of switches. Il1a and il2a are the current through the inductors L1 and L2. Ib is the battery current. Vdo1 is the voltage across the output diode Do1. Ido1 is the current flowing through Do1.

In mode 1 of the converter two 180˚ out of phase gate signal sharing equal duty ratio are applied to switches S1 and S2 respectively. And the other duty ratio is shared by the switches S3 and S4.switches S3 and S4 are operates in synchronous rectification mode with switches S1 & S2 respectively.

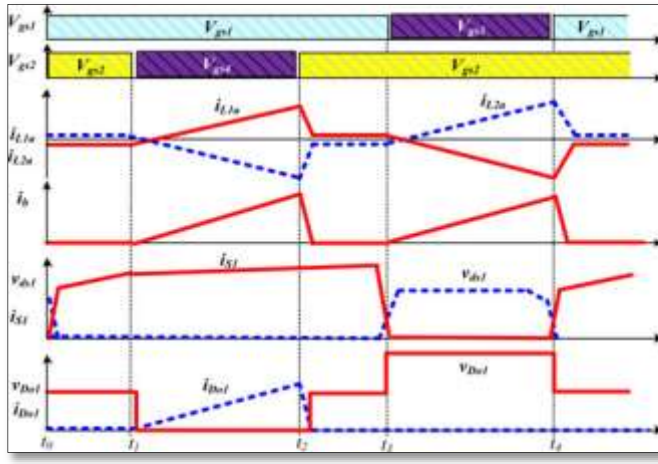

Figure 8- Key waveform of Mode1

State I [t0-t1]: both the switches are ON, the converter operates I fly-back mode to store the energy from PV.
State II [t1-t2]: at t1, the S2 turns OFF and S4 turns ON. The primary side of the inductor L2 charges the battery through S4 and during this state L1 operates in Forward mode and L2 operates in Fly-back mode.
State III [t2-t3]: at t2, S2 turns ON which makes the Switch S4 turns OFF and the converter operates in Fly-back mode to store energy.
State IV [t3-t4]: at t3, S1 turns OFF and S3 turns ON. The primary side of L1 charges the battery through S3. And L2 operates in forward mode to transfer energy from source to load.

In mode-2 operation the battery operates as the primary source of energy the switches S3 and S4 becomes the main switches to transfer the energy to the load while the S1 and S2 operates in their complementary manner.

In operational mode 3 of the converter in which no load is connected at the output port of the converter hence the whole energy generated by PV is directed towards the battery and during this period the switches S1 and S2 sharing equal duty ratio and having no phase shift between them are applied . And the switches S3 and S4 are kept OFF during this mode of operation.

Fig.15 describes the control scheme of the converter. The converter is controlled by the phase shift between the main switches S1 & S2, as the switches S3 & S4 operates in complementary manner. The output voltage and the MPPT can be regulated by the PS angle of the switches. For MPPT it is considered that the PV voltage is assigned to the 80% of VOC in the MPPT loop. Hence by varying the PS angle the duty cycle can be varied accordingly and therefore the Duty cycle is the only controlling variable for the converter.

By employing this control scheme to the converter the duty cycle is varied depending up on the modes of operation and smooth transition from one mode to other mode can be achieved.

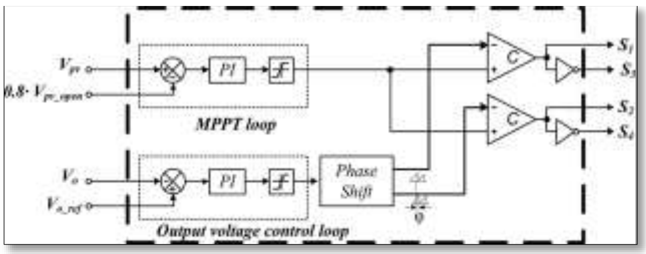

Figure 9- Control scheme of the converter

II. COMPARATIVE ANALYSIS

To ensure the integrity of all the converters they are simulated in the MATLAB environment for the 60 W ratings. The voltage input of the converter is made compatible to the battery ratings and resistive load is connected at the output port and based on the results a table formed to show the comparative analysis

Table 2- Comparative analysis of all the converter topologies

Sr No.	Parameters	Topology1	Topology2	Topology3
1.	Efficiency	Low	High	High
2.	Step-up ratio	Low	Low	High
3.	Galvanic isolation	Yes	Yes	Yes
4.	Component count	High	High	Low
5.	Overall Mass	High	High	Low
6.	Conversion stage	One	One	One
7.	Control Scheme	Complex	Complex	Relatively simple
8.	Control variables	High	High	Low
9.	MPPT controller	Required	Required	Not required

5. CONCLUSION

A study on the stand-alone photovoltaic systems is carried out in the paper. Conventionally requirement of two converters is overcome by employing the three port converter. A study carried out on Half Bridge topology, Full Bridge topology and a topology derived from Fly-back and forward topology. By analyzing all the converters and their operational modes it is found that the toplogy-3 found to be best suited for the stand-alone systems and still utilizing simple power electronics elements and simple control scheme while still making the converter cost effective and system is more efficient. Therefore, it can be concluded that this topology is well suitable for the Electric Vehicle charging purpose.

REFERENCES

[1] W. Xiao, A. Elnosh, V. Khadkikar, and H. Zeineldin, “Overview of maximum power point tracking technologies for photovoltaic power systems,” in Proc. IEEE 37th Annu. Conf. IEEE Ind. Electron. Soc., 2011, pp. 3900–3905.

[2] P. Bajpai and V. Dash, “Hybrid renewable energy systems for power generation in stand-alone applications: A review,” Renewable Sustainable Energy Rev., vol. 16, no. 5, pp. 2926–2939, 2012.

[3] H.Wu, R. Chen, J. Zhang, Y. Xing, H. Hu, and H. Ge, “A family of threeport half-bridge converters for a stand-alone renewable power system,” IEEE Trans. Power Electron., vol. 26, no. 9, pp. 2697–2706, Sep. 2011.

[4] H. Tao, J. L. Duarte, and M. A.M. Hendrix, “Three-port triple-half-bridge bidirectional converter with zero-voltage switching,” IEEE Trans. Power Electron., vol. 23, no. 2, pp. 782–792, Mar. 2008

[5] H. Tao, A. Kotsopoulos, J. L. Duarte, and M. A. M. Hendrix, “Family of multiport bidirectional DC-DC converters,” Proc. IEE Electric Power Appl., vol. 153, no. 3, pp. 451–458, May 2006.

[6] H. Wu, K. Sun, R. Chen, H. Hu, and Y. Xing, “Full-bridge three-port converters with wide input voltage range for renewable power systems,” IEEE Trans. Power Electron., vol. 27, no. 9, pp. 3965–3974, Sep. 2012.

[7] Z. Qian, O. Abdel-Rahman, H. Al-Atrash, and I. Batarseh, “Modeling and control of three-port DC/DC converter interface for satellite applications,” IEEE Trans. Power Electron., vol. 25, no. 3, pp. 637–649, Mar. 2010

[8] Y.Hu, W.Cao, B.Ji and J.Morrow “Three-port DC-DC converter for Stand-Alone Photovoltaic Systems” IEEE Transaction on Power Electronics, Vol.30, No.6, June 2015.